Mechanical Damage and Strain in Carbon Fiber Thermoplastic-Matrix Composite, Sensed by Electrical Resistivity Measurement

ZHEN MEI, VICTOR H. GUERRERO, DANIEL P. KOWALIK, *and* D. D. L. CHUNG

Composite Materials Research Laboratory
University at Buffalo
The State University of New York
Buffalo, NY 14260-4400

The volume electrical resistivity of a unidirectional continuous carbon fiber thermoplastic (nylon-6) matrix composite was found to be an indicator of strain and damage during repeated loading in the fiber direction. The through-thickness resistivity irreversibly and gradually decreased upon damage (probably fiber-matrix debonding) during repeated compression or tension. Moreover, it reversibly and abruptly increased upon matrix damage, which occurred reversibly near the peak stress of a stress cycle. In addition, the resistivity increased reversibly upon tension in every stress cycle, and decreased reversibly upon compression in every stress cycle. On the other hand, the longitudinal resistivity irreversibly and gradually increased upon damage. Moreover, it decreased reversibly upon tension in every stress cycle and increased reversibly upon compression in every stress cycle. The through-thickness resistivity was a better indicator of damage and strain than the longitudinal resistivity.

INTRODUCTION

Polymer-matrix composites with continuous carbon fibers are widely used for lightweight structures, such as aircraft, rotating machinery and sporting goods. Although thermoset-matrix composites are dominant, partly owing to their relatively long history of usage, thermoplastic-matrix composites are increasingly used because of their toughness and good hot/wet properties. Although toughness is associated with damage tolerance, the strategic applications associated with the use of advanced composites demand safety to a high degree. To avoid hazard due to damage, the monitoring of the damage (i.e., structural health monitoring) is necessary. Moreover, the damage mechanism needs to be investigated and the type of damage needs to be characterized, as such information is valuable for guiding the design and use of the composites.

Damage is conventionally detected by nondestructive methods such as ultrasonic and eddy current methods, which are carried out after the damage infliction rather than during the damage infliction. Observation after the damage infliction allows condition monitoring, whereas observation during the damage infliction enables better understanding of the cause, mechanism and nature of the damage. Moreover, observation after the damage infliction allows detection of irreversible effects, whereas observation during the damage infliction allows detection of both reversible and irreversible effects. A nondestructive method that is used during damage infliction is acoustic emission (1–4), but this technique does not give information on the reversibility of damage and tends to be sensitive to significant damage only. This paper uses a less common method, namely electrical resistance measurement, for observation during damage infliction (5–25).

The sensing of strain, including that in the elastic regime, is valuable to structural vibration control and load history recording. Moreover, the simultaneous sensing of strain and damage allows determination of the point of the dynamic stress variation at which damage occurs, thereby facilitating analysis of the cause of the damage. Owing to the reversibility of strain in the elastic regime, strain sensing requires a nondestructive method that is used in real time during the dynamic loading. A method that can provide damage sensing may not be able to provide strain sensing. An example of such a method is acoustic emission. This paper used electrical resistance measurement for sensing both strain and damage simultaneously.

Electrical resistance measurement has been previously used to sense strain and damage in carbon fiber thermoset (epoxy)-matrix composites. Tensile strain in the fiber (longitudinal) direction of the composite causes the electrical resistivity in the fiber direction to decrease and causes that in the through-thickness direction to increase, due to the increase in fiber alignment in the fiber direction. Damage in the form of fiber breakage causes the electrical resistivity in the fiber direction to increase, whereas damage in the form of delamination causes the resistivity in the through-thickness direction to increase. Hence, electrical resistance measurement allows simultaneous strain and damage sensing.

Fiber damage is a more drastic kind of damage than matrix damage, as the fibers are much stronger than the matrix and damage tends to involve the matrix before involving the fibers. Thus, in practical structures, matrix damage is more common than fiber damage.

Matrix damage affects the through-thickness resistance more than the resistance in the fiber direction (11). Previous work on the sensing of matrix damage in carbon fiber polymer-matrix composites by electrical resistance measurement involved measuring the through-thickness resistance during cyclic tension in the fiber direction of the composite (10, 11). The matrix was epoxy. Matrix damage was observed to start at a third of the fatigue life, as shown by an irreversible increase of the through-thickness resistance. In contrast, this work addresses the sensing of matrix damage during cyclic compression as well as cyclic tension in the fiber direction. As compression in the fiber direction is a mode of deformation that has high propensity for causing delamination, the study of damage under this mode of deformation is relevant.

EXPERIMENTAL METHODS

The thermoplastic polymer was nylon-6 (PA) in the form of unidirectional carbon-fiber (CF) prepregs supplied by Quadrax Corp. (Portsmouth, Rhode Island; QNC 4162). The fibers were 34–700 from Grafil, Inc. (Sacramento, California). The fiber diameter was 6.9 μm. The fiber weight fraction in the prepreg was 62%. The glass transition temperature (T_g) was 40–60°C and the melting temperature (T_m) was 220°C for the nylon-6 matrix. The prepreg thickness was 250 μm.

For preparing specimens for compressive testing, the prepreg was cut to size 76 × 38 mm. Then 108 plies of the prepreg were stacked in a steel mold. For preparing specimens for tensile testing, the prepreg was cut to size 180 × 125 mm. Then 6 plies of the prepreg were stacked in a steel mold. Either type of stack was heated to 260°C at a heating rate of 10°C/min and a pressure of 2.0 MPa. Then it was consolidated by hot pressing at 260°C and 2.0 MPa for 30 min. After demolding, the specimen was cut and polished to size 50 × 35 × 21 mm for the compressive specimens and size 180 × 13 × 1 mm for the tensile specimens.

The strain in the fiber (longitudinal) direction was measured by using a resistive strain gauge attached to the middle of one of the larger sides that were parallel to the fiber direction. The strain in the through-thickness direction was calculated by using the longitudinal strain and the Poisson ratio, which was 0.2 for the fiber and 0.33 for the matrix.

The volume electrical resistance R was measured using the four-probe method while cyclic compression or tension was applied in the longitudinal direction (*Figs. 1* and *2* for compression and tension respectively), using a screw-action mechanical testing system (Sintech 2/D). Silver paint was used for all electrical contacts. The four probes consisted of two outer current probes and two inner voltage probes. The separation of the current and voltage probes allowed elimination of the contact resistance from the measured resistance. The resistance R refers to the sample resistance between the inner probes. Longitudinal and through-thickness R values were measured in separate experiments. For the longitudinal R measurement, the four electrical contacts (A, B, C and D) were around the whole perimeter of the sample in four parallel planes that were perpendicular to the stress axis, such that the inner probes (B and C) were 30 mm apart and the outer probes (A and D) were 40 mm apart for compressive testing (*Fig. 1*), and the inner probes (B and C) were 110 mm apart and the outer probes (A and D) were 130 mm apart for tensile testing (*Fig. 2*). For the through-thickness R measurement, the current contacts (A′ and D′) were centered on the larger opposite

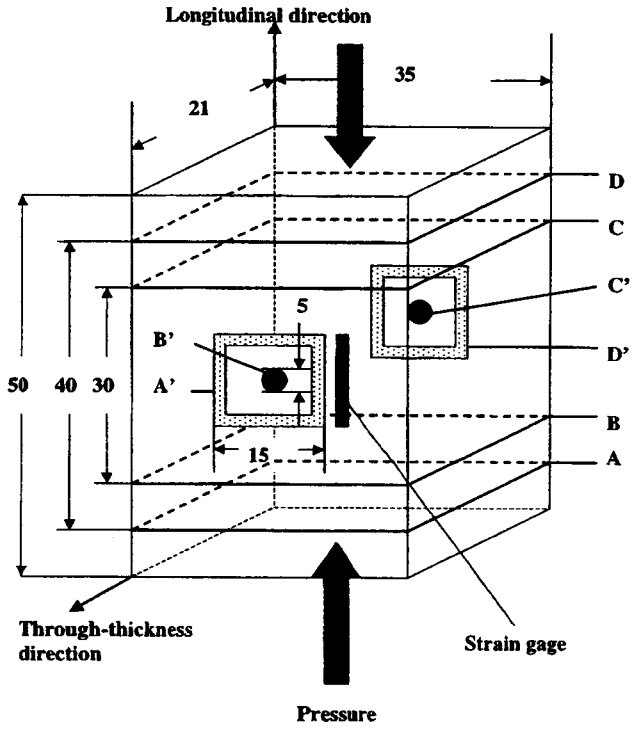

Fig. 1. Sample configuration for compressive testing. All dimensions are in mm. A, B, C and D are electrical contacts for longitudinal (stress direction; fiber direction) electrical resistivity measurement. A′, B′, C′ and D′ are electrical contacts for through-thickness electrical resistivity measurement.

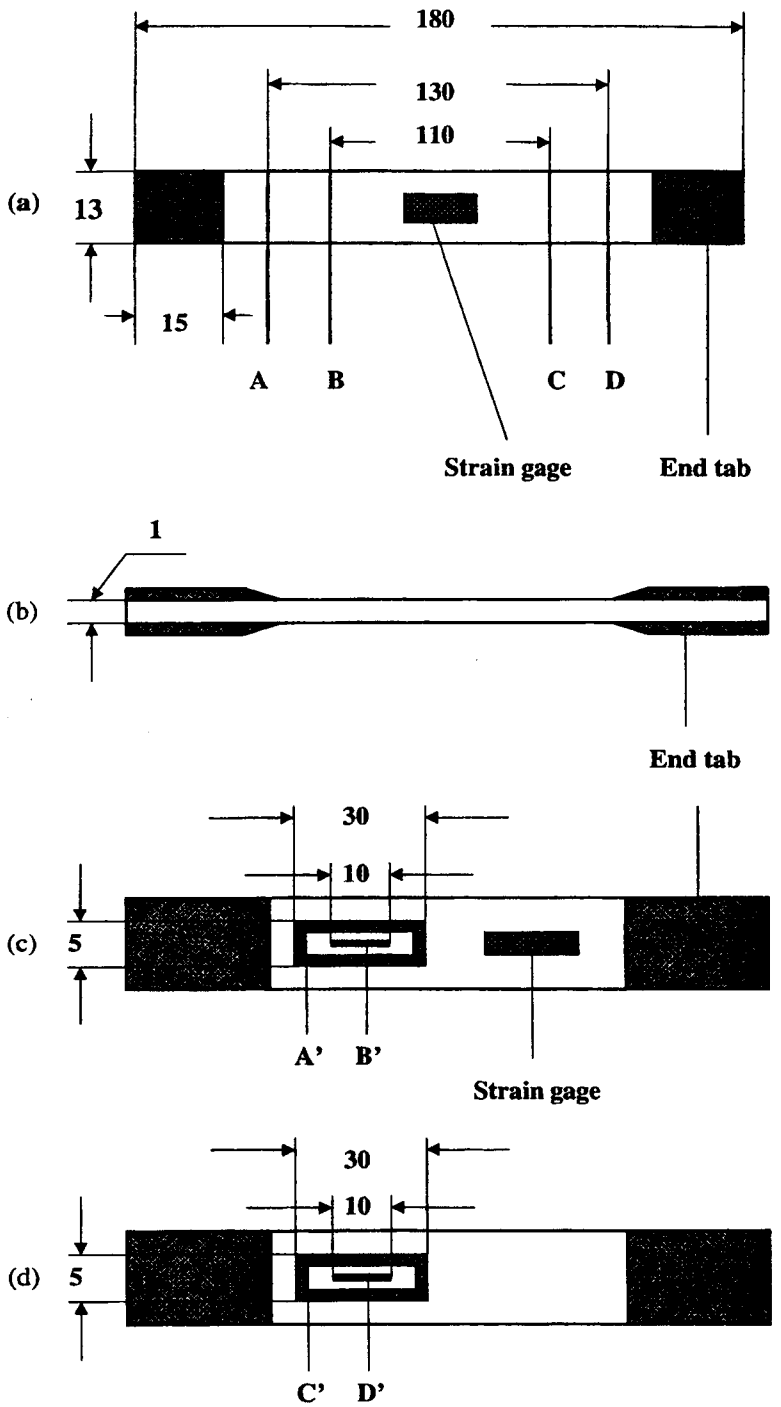

Fig. 2. Sample configuration for tensile testing. All dimensions are in mm. A, B, C and D are electrical contacts for longitudinal (stress direction; fiber direction) electrical resistivity measurement. A', B', C' and D' are electrical contacts for through-thickness electrical resistivity measurement. (a) and (c): Top view. (b): Side view. (d): Bottom view.

faces and in the form of open rectangles (length 15 mm in the fiber direction for compressive testing and 30 mm for tensile testing), while each of the two voltage contacts (B' and C') was in the form of a solid circle (diameter 5 mm) for compressive testing and a solid rectangle (10 mm long and 2 mm wide) for tensile testing, surrounded by a current contact (open rectangle). Thus, each face had a current contact surrounding a voltage contact (*Figs. 1* and *2*). A strain gauge was attached to one of these faces (*Figs. 1* and *2*). A Keithley 2001 multimeter was used.

The resistivity ρ was calculated from the measured resistance R and the strains in both longitudinal and through-thickness directions by using the equation

$$R = \rho \frac{\ell}{A} \quad (1)$$

where ℓ is the distance between the voltage probes in the direction of resistance measurement and A is the cross-sectional area perpendicular to the direction of resistance measurement. The ℓ relates to the longitudinal strain. The A relates to the transverse (through-thickness) strain. The temperature rise during the resistance measurement was negligible. The resistance measurement was nondestructive.

The damage revealed by resistance measurement was subtle, in contrast to damage in the form of well-defined delamination cracks or debonded regions at the fiber-matrix interface. Therefore, correlation of the resistance change with microscopic observation of damage was impossible.

RESULTS AND DISCUSSION

Compressive Testing

Figure 3 shows the fractional change in resistivity in the through-thickness direction during initial cyclic compression in the longitudinal (fiber) direction. The stress amplitude was 1.25 MPa for all cycles. (The compressive strength was 300 MPa in the longitudinal direction, as separately measured.) The resistivity decreased reversibly upon loading in every cycle, due to decrease in the degree of fiber alignment and the consequent increased chance of fibers of adjacent laminae touching one another. This resistivity decrease allows strain sensing. The fractional change in through-thickness resistivity (reversible portion only) per unit through-thickness strain (reversible portion only) is −2.3. The first three stress cycles were not used to calculate this fractional change, because a stabilized effect was of interest.

The resistivity baseline gradually decreased as cycling progressed, particularly in the first few cycles (*Fig. 3*), because of damage associated with plastic deformation (i.e., the occurrence of some irreversible strain, as shown in *Fig. 3*), which causes an irreversible increase of the chance for fibers of adjacent laminae to touch one another, thereby causing the resistivity to decrease irreversibly. Fiber-matrix debonding may occur to a small degree during the plastic deformation. The longitudinal strain is shown in *Fig. 3*.

As cycling progressed, the resistivity abruptly increased more and more around the peak stress of a cycle. This is attributed to matrix damage which occurred near the peak stress; the matrix damage decreased the chance for fibers of adjacent laminae to touch one another, thereby causing the through-thickness resistivity to increase. The resistivity increase was reversible, implying that the damage (e.g., microcrack opening) was subtle and reversible. The extent of damage increased as cycling progressed.

At a higher stress amplitude of 2.50 MPa, the through-thickness resistivity behaved similarly, except that the resistivity increase around the peak stress of a cycle was much larger (*Fig. 4*).

Figure 5 shows that the longitudinal resistivity increased reversibly upon cyclic compression in the longitudinal direction. The stress amplitude was 0.95 MPa. The resistivity increase is due to decrease in the degree of fiber alignment. The effect allows strain sensing. The fractional change in longitudinal resistivity (reversible portion) per unit longitudinal strain (reversible portion) is −0.6. The first three stress cycles were not used in calculating this fractional change, because a stabilized effect was of interest. The noise for the longitudinal resistivity variation (*Fig. 5*) is much higher than that for the through-thickness resistivity

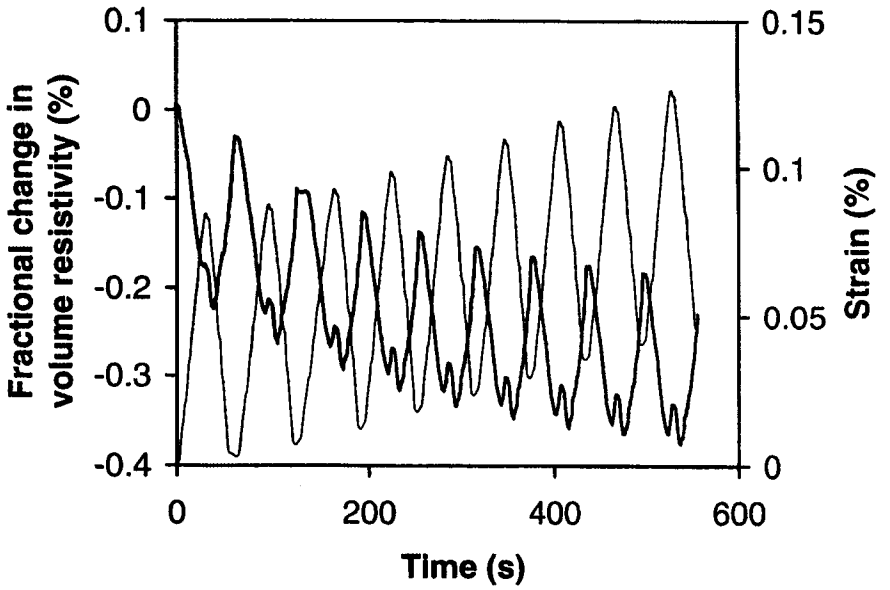

Fig. 3. Fractional change in through-thickness electrical resistivity (thick line) and through-thickness strain (thin line) during cyclic compressive loading at a stress amplitude of 1.25 MPa in the fiber direction.

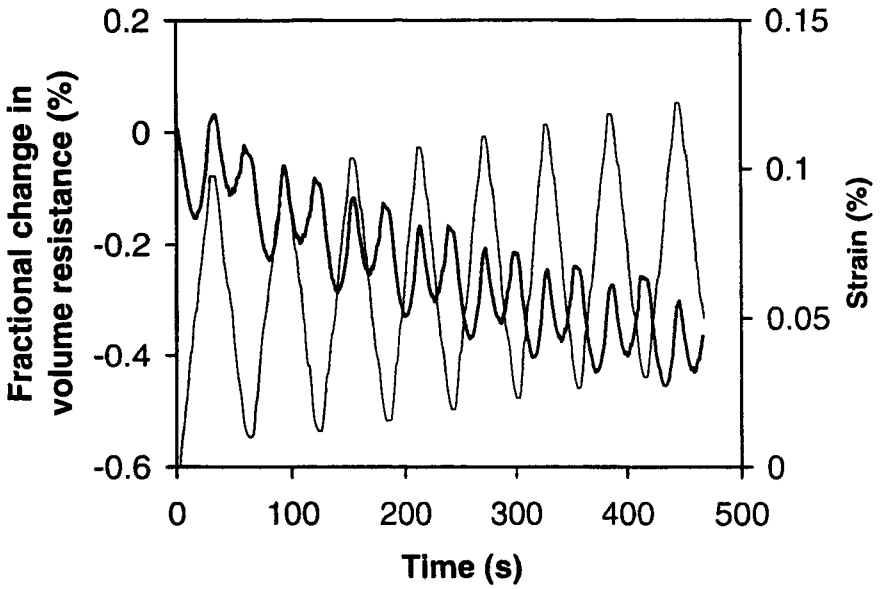

Fig. 4. Fractional change in through-thickness electrical resistivity (thick line) and through-thickness strain (thin line) during cyclic compressive loading at a stress amplitude of 2.50 MPa in the fiber direction.

variation (*Figs. 3* and *4*). Behavior similar to *Fig. 5* was observed at various stress amplitudes up to 3.2 MPa. Other than a slight increase of the resistivity baseline, no resistivity effect that could be attributed to damage was observed up to a stress amplitude of 3.2 MPa. Thus, the longitudinal resistivity was much less sensitive to damage than the through-thickness resistivity, as expected.

Tensile Testing

Figure 6 shows the fractional change in resistivity in the through-thickness direction during initial cyclic tension in the longitudinal (fiber) direction. The stress amplitude was 68.4 MPa for all the cycles. (The tensile strength was 1500 MPa in the longitudinal direction, as separately measured.) The resistivity increased reversibly upon loading in every cycle, owing to an increase in the degree of fiber alignment and the consequent decreased chance of fibers of adjacent laminae touching one another. This resistivity allows strain sensing. The fractional change in through-thickness resistivity (reversible portion) per unit through-thickness strain (reversible portion) ranges from −17 to −14, depending on the particular cycle after the first cycle, which was not used for calculating this fractional change.

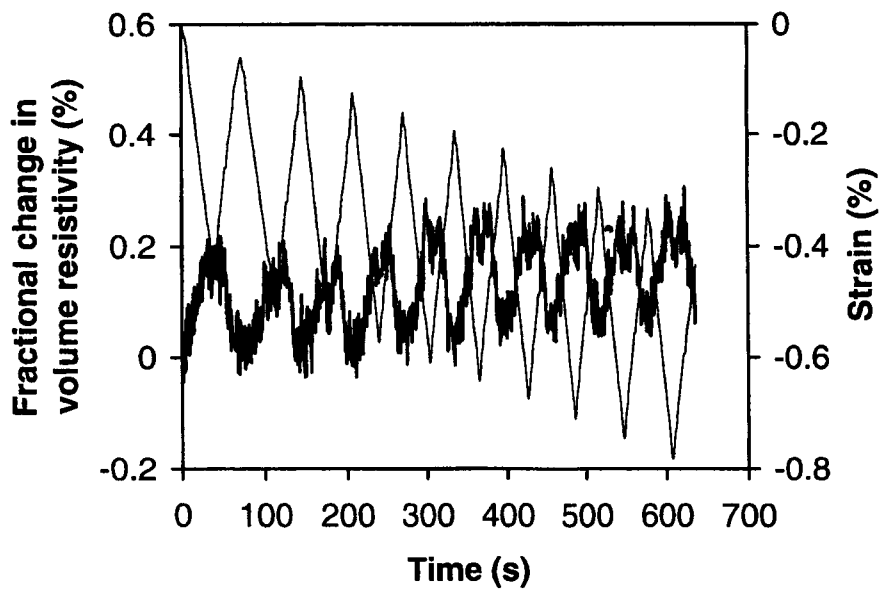

Fig. 5. Fractional change in longitudinal electrical resistivity (thick line) and longitudinal strain (thin line) during cyclic compressive loading at a stress amplitude of 0.95 MPa in the fiber direction.

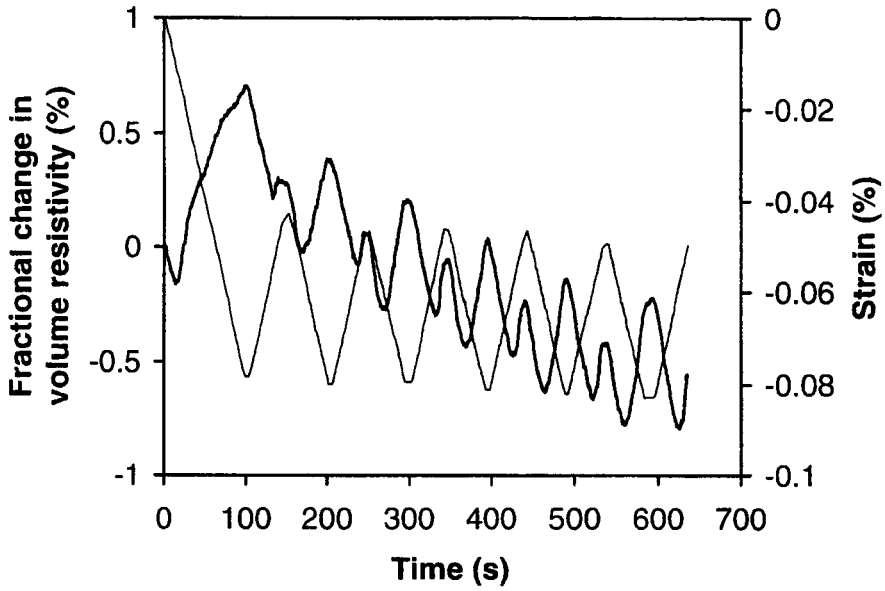

Fig. 6. Fractional change in through-thickness electrical resistivity (thick line) and through-thickness strain (thin line) during cyclic tensile loading at a stress amplitude of 68.4 MPa in the fiber direction.

The resistivity baseline (*Fig. 6*) gradually decreased as cycling progressed, as in *Fig. 3* (compression), owing to damage that caused an irreversible increase of the chance for fibers of adjacent laminae to touch one another. The longitudinal strain shown in *Fig. 7* shows partial reversibility of the strain after the first cycle and a gradual and slight increase of the strain baseline as cycling progressed. This means that the irreversible portion of the strain increased slightly upon cycling. Hence, plastic deformation was most significant in the first cycle, though additional plastic deformation occurred as cycling progressed. The damage is related to the plastic deformation and is probably in the form of fiber-matrix debonding.

As cycling progressed, the resistivity abruptly increased more and more around the peak stress of a cycle (*Fig. 6*), as in *Fig. 3* (compression). This is attributed to matrix damage, which occurred near the peak stress and caused the through-thickness resistivity to increase. The resistivity increase was reversible,

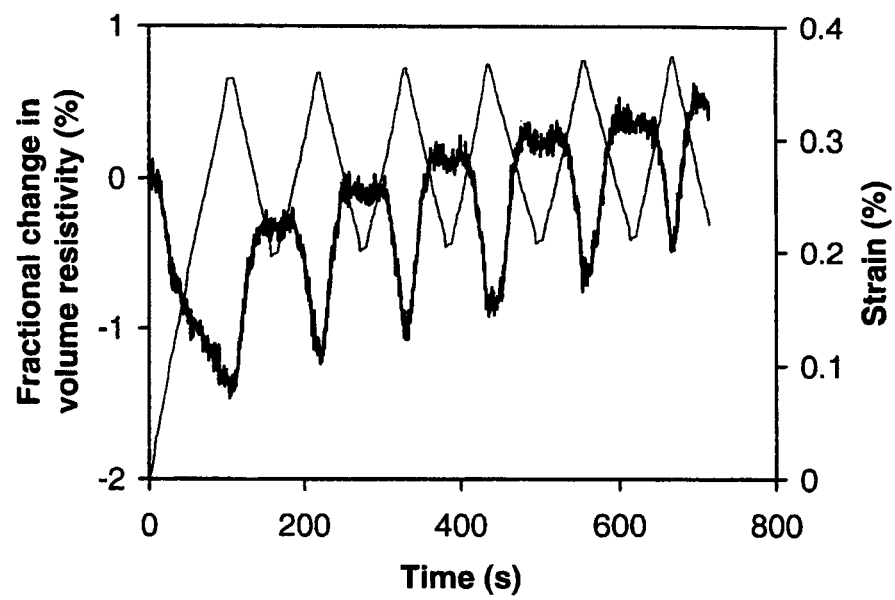

Fig. 7. Fractional change in longitudinal electrical resistivity (thick line) and longitudinal strain (thin line) during cyclic tensile loading at a stress amplitude of 68.4 MPa in the fiber direction.

implying that the damage was subtle and reversible. The extent of damage increased as cycling progressed, as shown by the greater extent of resistivity increase at the peak stress of a cycle. This damage effect was ignored in calculating the fractional change in resistivity per unit strain given above (ranging from −17 to −14).

At a higher stress amplitude of 171.1 MPa, the through-thickness resistivity and strain behaved similarly, except that the fractional change in resistivity and the strain were much higher (*Fig. 8* in comparison to *Fig. 6*).

Figure 7 shows that the longitudinal resistivity decreased reversibly upon cyclic tension in the longitudinal direction. The stress amplitude was 68.4 MPa. The resistivity decrease is due to increase in the degree of fiber alignment. The effect allows strain sensing. The fractional change in longitudinal resistivity (reversible portion) per unit longitudinal strain (reversible portion) is −6.2. The first stress cycle was not used in calculating this fractional change, because it involved much irreversible strain.

As cycling progressed, the longitudinal resistivity baseline gradually increased. This is due to plastic deformation (as shown by the partly irreversible strain, *Fig. 7*) and the resulting damage, probably in the form of fiber-matrix debonding.

At a higher stress amplitude of 136.9 MPa, the longitudinal resistivity and strain behaved similarly, except that the fractional change in resistivity and the strain were higher (*Fig. 9*).

The noise for the longitudinal resistivity variation (*Figs. 7* and *9*) is higher than that for the through-thickness resistivity (*Figs. 6* and *8*), as in the case of compressive testing. This is due to the lower resistivity in the longitudinal direction.

Comparison

Comparison of *Fig. 7* (tension) and *Fig. 5* (compression) in terms of the increase in resistivity baseline shows that the longitudinal resistivity is sensitive to damage under tension, but not very sensitive to damage under compression. However, comparison of *Figs. 6* and *8* (tension) and *Figs. 3* and *4* (compression) shows that the through-thickness resistivity is sensitive to damage under tension as well as damage under compression.

The fractional change in resistivity per unit strain (whether longitudinal or through-thickness) is higher for tension than compression. This means that tension has more effect on the degree of fiber alignment than compression. Whether under tension or compression, the fractional change in resistivity per unit strain is higher in magnitude in the through-thickness direction than the longitudinal direction. This has to do with the lower strain magnitude in the through-thickness direction than in the longitudinal direction.

Together with the fact that the noise is greater for the longitudinal resistivity than for the through-thickness resistivity, the above two paragraphs mean that the through-thickness resistivity is a better indicator of damage and strain than the longitudinal resistivity.

The results of this work are consistent with earlier results on carbon fiber epoxy-matrix composites (6, 7, 9–13) in relation to the effect of reversible strain on the resistivity and the effect of matrix damage on the resistivity, even though the earlier results were obtained during repeated tension only. However, the matrix damage observed in the epoxy case was irreversible, whereas it was reversible in the thermoplastic case of this work. Moreover, the plastic deformation and the irreversible and gradual damage (as indicated by the increase in resistivity baseline) observed in the

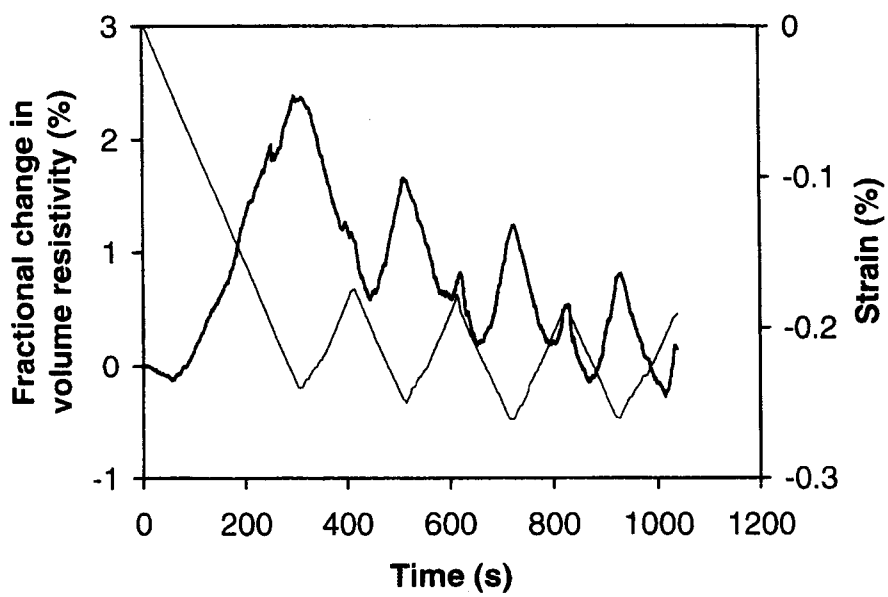

Fig. 8. Fractional change in through-thickness electrical resistivity (thick line) and through-thickness strain (thin line) during cyclic tensile loading at a stress amplitude of 171.1 MPa in the fiber direction.

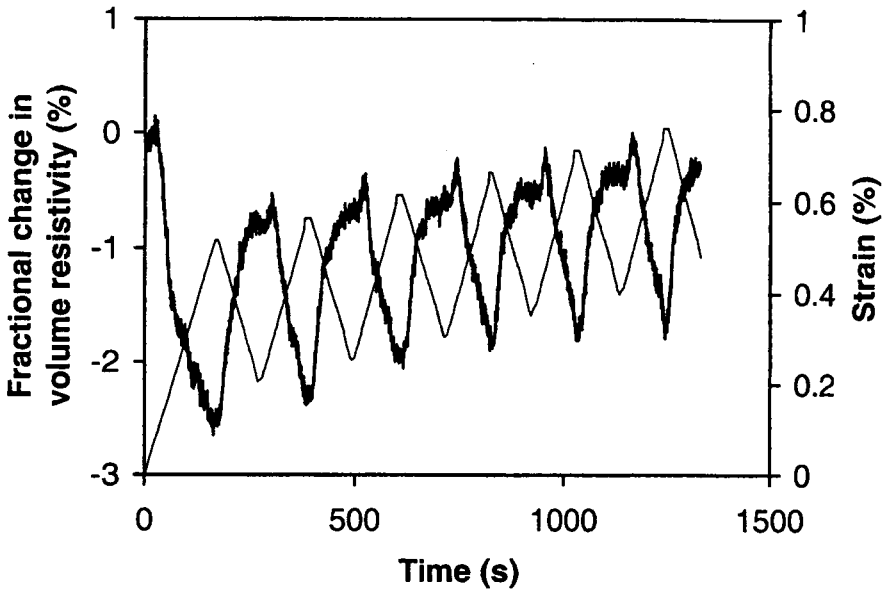

Fig. 9. Fractional change in longitudinal electrical resistivity (thick line) and longitudinal strain (thin line) during cyclic tensile loading at a stress amplitude of 136.9 MPa in the fiber direction.

thermoplastic case (probably due to fiber-matrix debonding) were not observed in the epoxy case. These differences between the two cases are consistent with the crosslinked structure and brittleness of the epoxy matrix.

CONCLUSION

The through-thickness and longitudinal volume electrical resistivity of a unidirectional continuous carbon fiber nylon-6 matrix composite was found to indicate strain and damage when the composite was under repeated compression or tension in the fiber direction. Both resistivities changed reversibly upon loading, because of a change in the degree of fiber alignment upon loading, thereby providing a mechanism of strain sensing. In addition, both resistivities irreversibly and gradually changed upon damage (probably fiber-matrix debonding that accompanied plastic deformation) which irreversibly increased the chance of fibers of adjacent laminae to touch one another. Moreover, the through-thickness resistivity reversibly and abruptly increased upon matrix damage, which occurred reversibly near the peak stress of a cycle. Both types of damage increased in extent as stress cycling progressed.

REFERENCES

1. M. Fuwa, B. Harris, and A. R. Bunsell, *J. Phys. D.*, **8**, 1460 (1975).
2. M. Fuwa, A. R. Bunsell, and B. Harris, *J. Strain Analysis*, **11**, 97 (1976).
3. M. Fuwa, A. R. Bunsell, and B. Harris, *J. Phys. D.*, **9**, 353 (1976).
4. M. Fuwa, A. R. Bunsell, and B. Harris, *J. Mater. Sci.*, **10**, 2062 (1975).
5. N. Muto, H. Yanagida, T. Nakatsuji, M. Sugita, Y. Ohtsuka, and Y. Arai, *Smart Mater. Struct.*, **1**, 324 (1992).
6. X. Wang, X. Fu, and D. D. L. Chung, *J. Mater. Res.*, **14**(3), 790 (1999).
7. X. Wang and D. D. L. Chung, *Composites: Part B*, **29B**(1), 63 (1998).
8. P. E. Irving and C. Thiogarajan, *Smart Mater. Struct.*, **7**, 456 (1998).
9. X. Wang and D. D. L. Chung, *J. Mater. Res.*, **14**(11), 4224 (1999).
10. X. Wang and D. D. L. Chung, *Polymer Composites*, **18**(6), 692 (1997).
11. S. Wang and D. D. L. Chung, *Polymer Composites*, in press.
12. S. Wang and D. D. L. Chung, *Polymer Composites*, **21**(1), 13 (2000).
13. X. Wang, S. Wang, and D. D. L. Chung, *J. Mater. Sci.*, **34**(11), 2703 (1999).
14. N. Muto, H. Yanagida, M. Miyayama, T. Nakatsuji, M. Sugita, and Y. Ohtsuka, *J. Ceramic Soc. Japan*, **100**(4), 585 (1992).
15. N. Muto, H. Yanagida, T. Nakatsuji, M. Sugita, Y. Ohtsuka, Y. Arai, and C. Saito, *Adv. Composite Mater.*, **4**(4), 297 (1995).
16. R. Prabhakaran, *Experimental Techniques*, **14**(1), 16 (1990).
17. M. Sugita, H. Yanagida, and N. Muto, *Smart Mater. Struct.*, **4**(1A), A52 (1995).
18. A. S. Kaddour, F. A. R. Al-Salehi, S. T. S. Al-Hassani, and M. J. Hinton, *Composites Sci. Tech.*, **51**, 377 (1994).
19. O. Ceysson, M. Salvia, and L. Vincent, *Scripta Materialia*, **34**(8), 1273 (1996).
20. K. Schulte and Ch. Baron, *Composites Sci. Tech.*, **36**, 63 (1989).
21. K. Schulte, *J. Physique I*, **3**(7), 1629 (1993).
22. J. C. Abry, S. Bochard, A. Chateauminois, M. Salvia, and G. Giraud, *Composites Sci. Tech.*, **59**(6), 925 (1999).
23. A. Todoroki, H. Kobayashi, and K. Matuura, *JSME Int. J. Series A—Solid Mechanics Strength of Materials*, **38**(4), 524 (1995).
24. S. A. Hayes, D. Brooks, T. Liu, S. Vickers, and G. F. Fernando, *Proc. SPIE—the Int. Soc. for Optical Engineering*, V. 2718 (Smart Structures and Materials 1996: Smart Sensing, Processing, and Instrumentation), SPIE, Bellingham, WA, 1996, p. 376–384.
25. S. Wang and D. D. L. Chung, *Polymers & Polymer Composites*, **9**(2), 135 (2001).